The Reaction of HCCO + O_2: Experimental Evidence of Prompt CO_2 by Time-Resolved Fourier Transform Spectroscopy

David L. Osborn*

Combustion Research Facility, Mail Stop 9055, Sandia National Laboratories, Livermore, California 94551-0969

Received: December 9, 2002; In Final Form: February 20, 2003

The products CO and CO_2 are observed experimentally for the first time in the HCCO + O_2 reaction. Both product molecules have identical appearance times and are formed simultaneously rather than sequentially. Both CO and CO_2 are produced with significant internal excitation. The product channel producing H + CO + CO_2 accounts for at least 90% of the reaction products at 298 K. The results explain the observation of "prompt" CO_2 in acetylene oxidation chemistry.

1. Introduction

The oxidation of acetylene is an important reaction in combustion of aliphatic[1] and aromatic[2] hydrocarbons. Shock tube experiments on the ignition of $C_2H_2/O_2/Ar$ mixtures[3] show formation of "prompt" CO_2, meaning that CO_2 is formed with the same time constant as CO. This observation implies that one of the reactants in the reaction(s) producing CO and CO_2 must be either C_2H_2 or O_2, which are present in high concentrations, and rules out formation of CO_2 via the reaction CO + OH → CO_2 + H, in which both reactants are intermediates. On the basis of experiments in lean C_2H_2/O_2 flames, Erberius et al.[4] suggested the reaction sequence

$$O + C_2H_2 \rightarrow {}^3CH_2 + CO \quad (1a)$$

$$^3CH_2 + O_2 \rightarrow CO_2 + H + H \quad (2)$$

which could explain prompt CO_2 formation. This reaction sequence predicts identical time constants for CO and CO_2 formation because $k_2 > k_{1a}$, and because O_2 is present in great excess (97% mole fraction). However, it is now generally agreed that reaction 1a is only a minor channel in the O + C_2H_2 reaction.[5]

In a recent theoretical paper, Klippenstein, Miller, and Harding[6] proposed a new pathway for prompt CO_2 formation in acetylene combustion:

$$O + C_2H_2 \rightarrow HCCO + H \quad (1b)$$

$$HCCO + O_2 \rightarrow H + CO + CO_2 \quad \Delta H_0 = -110.6 \text{ kcal/mol} \quad (3a)$$

$$\rightarrow OH + CO + CO \quad \Delta H_0 = -85.7 \text{ kcal/mol} \quad (3b)$$

Their calculation of the potential energy surface, along with direct dynamics trajectory simulations and master equation calculations, predicted that H + CO + CO_2 is the major product channel (∼90%) of reaction 3. In this paper, we report the first direct observation of products from the HCCO + O_2 reaction. The data support the conclusion in ref 6 that H + CO + CO_2 is the major product channel of HCCO + O_2 and give credence to this explanation of prompt CO_2 formation in acetylene oxidation.

There are four reports of kinetics measurements of the HCCO + O_2 reaction, all by monitoring the disappearance of the HCCO reactant.[7−10] At 296 K, Peeters *et al.*[7] measured the rate coefficient $k_3 = 6.3 \times 10^{-13}$ cm^3 molecule^{-1} s^{-1} by discharge flow mass spectrometry. Temps *et al.*[8] used far-infrared laser magnetic resonance to monitor HCCO, obtaining $k_3 = 2.2 \pm 0.7 \times 10^{-13}$. Murray *et al.*[9] observed HCCO by infrared kinetic spectroscopy, measuring $k_3 = 6.5 \pm 0.6 \times 10^{-13}$. Finally, Carl *et al.*[10] used photodissociation of HCCO followed by LIF on the CH ($X\ ^2\Pi$) fragment to obtain $k_3 = 8.6 \pm 0.4 \times 10^{-13}$. Reaction 3b was tentatively suggested as the most likely product channel on the basis of indirect observations in these experiments.[9,11]

2. Experimental Section

The reaction of HCCO + O_2 is monitored by step-scan, time-resolved Fourier transform emission spectroscopy[12] (TR-FTS). This multiplexed technique allows acquisition of broad-band, time-resolved spectra of multiple reactants and products simultaneously.

The reaction is initiated in a Teflon-coated stainless steel flow cell equipped with multipass collection optics. HCCO radicals are produced by 193 nm photolysis (26 mJ cm^{-2} pulse^{-1}, 50 Hz repetition rate) of ethyl ethynyl ether ($HCCOCH_2CH_3$), which has an absorption cross section $\sigma(193) \sim 7 \times 10^{-18}$ cm^2/molecule (base e), and produces HCCO + C_2H_5 with near unit quantum yield.[13] Ethyl ethynyl ether is commercially available as a 40% solution in hexane and is used without further purification. The hexane stabilizer is verified to have a negligible absorption cross section at 193 nm ($< 3 \times 10^{-22}$ cm^2/molecule) and therefore does not affect radical production. The sample is seeded in a small flow of helium (20 sccm) and combined with larger flows of He (99.999%) and O_2 (99.99%) (725 sccm combined flow), which enter the flow cell 1 cm above the photolysis beam. All flows are controlled by mass flow controllers. The cell is pumped by a roots blower, and the total cell pressure is maintained at 1.1 Torr by a closed-loop feedback valve throttling the pump. The flow rate is sufficient to flush the cell between laser pulses. As a consequence of this high flow rate, pump out losses contribute to signal decay during

* Tel: +1-925-294-4622. Fax: +1-925-294-2276. E-mail: dlosbor@sandia.gov.

10.1021/jp022571e CCC: $25.00
Published on Web 04/22/2003

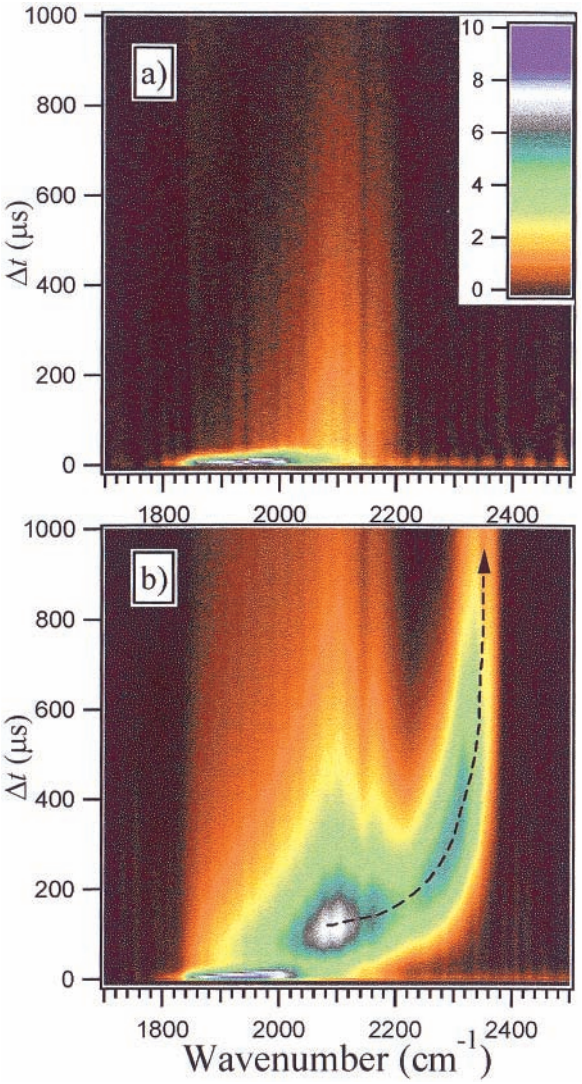

Figure 1. Image plots of time-resolved emission from photolysis of $HCCOCH_2CH_3$ (a) without O_2, and (b) with 4.2×10^{15} molecules cm^{-3} O_2. The dashed line in (b) denotes the maximum intensity of CO_2 emission as a function of time.

the 1.5 ms observation time of the experiment. A small flow of helium (100 sccm) purges the input and output photolysis windows to prevent photochemistry at these windows.

Transient infrared emission is collected by gold-coated Welsh-type multipass optics and exits the reaction cell through a BaF_2 window. The emission is collimated and refocused by a pair of off-axis parabolic mirrors in a nitrogen-purged environment before entering the evacuated step-scan Fourier spectrometer (Bruker 66v/S). The emission passes through the interferometer and is focused onto a liquid nitrogen-cooled InSb photodiode. The photodiode amplifier has a rise time of ~ 1 μs. For each optical path difference of the interferometer, the transient emission is digitized at 5 μs intervals. The resulting time-resolved interferograms are Fourier transformed to yield time-resolved survey spectra at 8 cm^{-1} resolution or time-resolved rovibrational spectra at 0.25 cm^{-1} resolution.

3. Results and Discussion

The antisymmetric CCO stretch (ν_2) in HCCO was first observed by Jacox and Olson[14] in an argon matrix at 2020 cm^{-1}. This band was rotationally resolved in the gas phase by Unfried et al.,[15] who assigned the band origin at 2023 cm^{-1}. Figure 1a shows a sequence of 200 time-resolved FTIR emission spectra

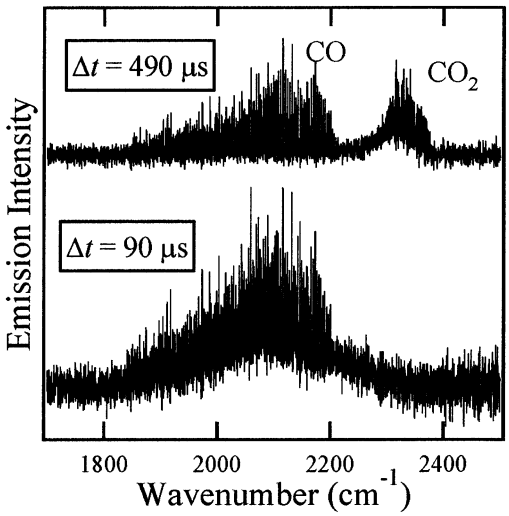

Figure 2. Time-resolved emission from HCCO + O_2. At 90 μs after photolysis the CO_2 emission forms a broad baseline on which the CO lines are superimposed. At 490 μs, rotationally resolved lines in both species can be seen.

(8 cm^{-1} resolution) arising from photodissociation of $HCCOCH_2$-CH_3 in the absence of O_2. Immediately following the excimer pulse ($t = 0$), emission is seen from 1800 to 2040 cm^{-1} and is assigned to $\Delta v_2 = -1$ bands of HCCO. The broad width and red-shifted mean wavenumber of this band indicate that HCCO is born with large amounts of vibrational excitation. With increasing time, the spectrum blue-shifts toward the band origin as the more energetic vibrational states are depopulated by collisional energy transfer. Weak emission from vibrationally excited CO is also seen from 1950 to 2200 cm^{-1}. Like the HCCO emission, CO is also observed with a detector-limited rise time and is unambiguously identified at higher resolution (0.25 cm^{-1}), where rotationally resolved bands from $v' = 1-8$ can be assigned and their population quantified. The laser intensity dependence of this CO shows that it is primarily produced by secondary photodissociation of HCCO at 193 nm to yield CH + CO,[16] although a small fraction of the CO might arise from unimolecular dissociation of nascent HCCO radicals.

Figure 1b shows spectra taken under identical conditions except for the replacement of 4.2×10^{15} molecules/cm^3 of He with O_2. Whereas emission from HCCO is nearly identical to that in Figure 1a, strong emissions are now observed from both CO (1900−2200 cm^{-1}) and CO_2 (1850−2370 cm^{-1}), which rise to maximum intensity by ~ 100 μs and slowly decay thereafter. Both product molecules are formed with significant internal excitation, leading to broad, red-shifted spectra at early times. Cooling of the CO_2 vibrational distribution by collisional energy transfer is manifested in the prominent ridge identified in Figure 1b that leads to the asymptotic wavenumber (2349 cm^{-1}) of the CO_2 (0001 → 0000) transition by 800 μs. At increased spectral resolution (0.25 cm^{-1}), both CO and CO_2 can be unambiguously identified from their rotationally resolved spectra, as shown in Figure 2 for two particular time slices. At 90 μs after the excimer flash, rovibrational bands of CO ($v' = 1-11$) are seen on top of broad CO_2 emission centered at 2100 cm^{-1}. At this early time in the reaction, the density of CO_2 transitions in the $(m,n,p) \rightarrow (m,n,p\text{-}1)$ bands, with many m and n levels populated, exceeds the inverse of the Doppler line width. This high transition density makes rotational structure of CO_2 unresolvable at early times regardless of experimental resolution. As the carbon dioxide undergoes vibrational energy transfer its broad emission shifts gradually and monotonically to the blue, until at 490 μs it is completely separated from the CO bands.

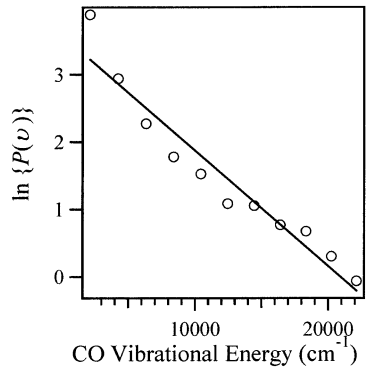

Figure 3. Boltzmann plot of the vibrational distribution of CO from HCCO + O_2. The straight line is the best fit of the data to a Boltzmann distribution with a temperature of 8400 ± 800 K.

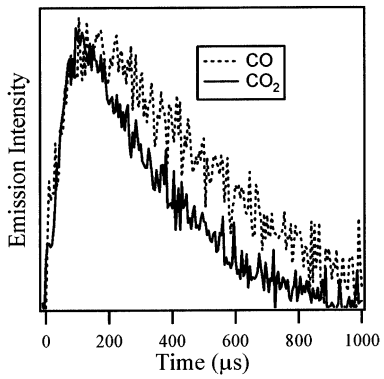

Figure 4. Integrated emission intensity as a function of time for the CO and CO_2 products with $[O_2] = 4.2 \times 10^{15}$ molecules cm^{-3}.

At this late time there are only a few vibrational levels of CO_2 populated, and single rotational lines in the asymmetric stretch manifold can be clearly identified.

To further quantify the energy disposal in this system, the intensities of the rotationally resolved CO lines are fit to literature line positions using a nonlinear least-squares routine. The fit gives a band intensity and rotational temperature for each upper vibrational state. The rotational temperatures are 300 ± 50 K for all bands, with branching ratios $v' = 1-11$ of 49:19:10:5.9:4.6:3.0:2.9:2.2:2.0:1.4:0.9. Because this fit was done for $\Delta t = 490$ μs (where the CO_2 baseline no longer contributes), these vibrational branching fractions are slightly colder than the nascent distributions. A Boltzmann plot of the CO vibrational intensities is given in Figure 3. The best fit to this distribution is described by a temperature $T_{vib}(CO) = 8400 \pm 800$ K.

The rovibrationally resolved TR-FTS data set, from which the two spectra in Figure 2 are extracted, can be used to compare the rise time of emission from CO and CO_2. A data set taken without O_2 is first subtracted from the data acquired with O_2 to remove emission from HCCO and photolytically generated CO. Because vibrational energy transfer in CO is very slow, the temporal profile of CO emission can be taken as the integrated area of the R7 line of the $1 \rightarrow 0$ band, and is shown in Figure 4. The integrated emission from CO_2 is obtained from the data in Figure 2 by extracting a low-resolution spectrum that contains contributions only from CO_2. This extraction is done by judiciously choosing wavenumbers in the range of 1800−2400 cm^{-1} that lie between the sharp CO lines. The low-resolution spectrum so constructed contains contributions only from CO_2 at all times, and the area under this curve is plotted as a function of time in Figure 4. Note, however, that the integrated emission for CO_2 is not related by a simple proportionality constant to the CO_2 concentration, as discussed below. Nevertheless, at early time the signals are proportional to concentration, and it can be seen that the rise times are identical within experimental error, providing evidence that CO and CO_2 are formed simultaneously as a result of reaction 3. Of course, the time constant for the rise of all products from all channels in reaction 3 will be equal to the time constant for the decrease of HCCO. Therefore, the common rise times of CO and CO_2 give no information about the branching ratio $k_{3b}/(k_{3a} + k_{3b})$. The common rise times do eliminate the possibility that reaction 3b is the dominant channel and CO_2 is formed in the secondary reaction OH + CO → H + CO_2. The fall times of the emission in Figure 4 are not identical and are a complicated function of collisional energy transfer and removal from the observation zone, as discussed below.

To address the kinetics of product formation, we estimate the precursor concentration in this study was $[HCCOCH_2CH_3] \sim 3 \times 10^{14}$ molecules/cm^3. The attenuation of the 193 nm photolysis laser was <2%. Therefore we estimate that $[HCCO]_0 = [C_2H_5]_0 \leq 5 \times 10^{13}$ molecules/cm^3. (Note that $C_2H_5 + O_2$ does not produce CO or CO_2).[17] The concentration range of $[O_2] = 8 \times 10^{14} - 1 \times 10^{16}$ molecules/cm^3 is sufficiently in excess to ensure pseudo-first-order conditions for all the data acquired. The rate of rise of CO and CO_2 formation from reaction 3 is therefore given by $k' = k_3[O_2]$. While the data in Figure 4 show that the rise time of the two products are identical, extraction of a product concentration profile from the TR-FTS data is complicated by two factors. First, vibrational energy transfer causes sequential deexcitation of both species, primarily by $\Delta v = -1$ transfers. Since the transition dipole moment is proportional to v', the observed emission is not simply proportional to concentration, but decreases with time as the molecules cool due to collisions. Second, product molecules in their zero-point level (or for CO_2, those with $v_3 = 0$) will not be detected by emission spectroscopy. Both of these complications are minimized at early time, when vibrational energy transfer has not altered the quantum state distributions too drastically. Bearing in mind these caveats, the initial rise of the product emissions are consistent with $k_3 \sim 6-8 \times 10^{-13}$ cm^3 $molecule^{-1}$ s^{-1} for all O_2 concentrations.

The high intensity and time evolution of the CO_2 emission is strong evidence that direct formation of H + CO + CO_2 is an important product channel of the title reaction. Extracting an absolute branching ratio from the data is not possible because there is no spectral evidence of the OH fragment from channel 3b in the 3300−3600 cm^{-1} range. Nevertheless, an upper limit on the branching fraction to OH + CO + CO can be obtained from this experiment. Two methods were used to determine this limit. The first method evaluates the detection sensitivity of OH on the $\Omega = 3/2 \rightarrow 3/2$ $Q(1.5)$ $v' = 1 \rightarrow 0$ transition at 3568.4 cm^{-1}, which is the strongest OH emission line for a 298 K rotational distribution. The reaction of $O(^1D)$ with methane provided the reference reaction for OH production:

$$N_2O + h\nu(193\text{ nm}) \rightarrow O(^1D) + N_2 \quad \Phi\{O(^1D)\} = 100\% \tag{4}$$

$$O(^1D) + N_2O \rightarrow \text{products} \qquad k_5 = 1.16 \times 10^{-10}\ cm^3\ molecule^{-1}\ s^{-1} \tag{5}$$

$$O(^1D) + CH_4 \rightarrow OH(v) + CH_3 \qquad k_{6a} = 1.13 \times 10^{-10}\ cm^3\ molecule^{-1}\ s^{-1} \tag{6a}$$

$$\rightarrow \text{other products} \qquad k_{6b} = 3.75 \times 10^{-11}\ \text{cm}^3\ \text{molecule}^{-1}\ \text{s}^{-1} \quad (6b)$$

where the quantum yield and rate coefficients[18] are at 298 K and the fraction of OH($v' = 1$) is 25%.[19] Assuming $[HCCO]_0 = 4 \times 10^{13}$ molecules/cm^3, a thermalized OH rotational distribution at 298 K and an OH vibrational distribution from reaction 3b similar to that from reaction 6a, the minimum detectable total OH density is 1.8×10^{12} molecules cm^{-3}, which places an upper limit on $k_{3b}/k_3 \leq 5\%$, where $k_3 = k_{3a} + k_{3b}$. The two major sources of uncertainty in this limit are the precision with which $[HCCO]_0$ is known and the assumption that the vibrational distributions of OH are identical in the reference reaction and HCCO + O_2.

The second method for calculating the branching fraction limit k_{3b}/k_3 is more reliable because it is independent of the initial HCCO number density. This method is based on comparison of the signal-to-noise of a CO emission line with the noise in the spectrum at the wavenumber of the OH line mentioned above. The ratio of total CO to OH is given by

$$\frac{\rho_{CO}}{\rho_{OH}^{lim}} = \frac{I_{CO} A_{OH} F_{OH}^{v'} F_{OH}^{J'}}{N_{OH} A_{CO} F_{CO}^{v'} F_{CO}^{J'}} = \frac{k_{3a} + 2k_{3b}}{k_{3b}} = \frac{k_3 + k_{3b}}{k_{3b}} \quad (7)$$

where ρ are total number densities, ρ_{OH}^{lim} is the limiting density of OH which would give a signal-to-noise ratio of unity, I_{CO} and N_{OH} are the emission signal and noise floor, respectively, for $v' = 1$ CO and OH rovibrational lines, respectively, A values are Einstein spontaneous emission coefficients for CO[20] and OH,[21] and the F values are Boltzmann fractions in the upper states for vibration and rotation. The rotational Boltzmann fractions are relaxed to 300 K under the conditions of the experiment, while the vibrational fraction for CO is determined from the data and that for OH is varied as discussed below. The branching fraction is given by

$$\frac{k_{3b}}{k_3} \leq \left(\frac{\rho_{CO}}{\rho_{OH}^{lim}} - 1 \right)^{-1} \quad (8)$$

Because the branching fraction determined by method 2 is independent of $[HCCO]_0$, the major uncertainty depends on the assumed vibrational distribution of the OH produced in channel 3b. As this channel is highly exothermic, it is unlikely that OH would be produced with no vibrational excitation. Since the CO vibrational distribution can be fairly well described as a Boltzmann distribution with $T_{vib}(CO) \sim 8400$ K, it is plausible that a vibrational temperature would also describe OH if it were produced. Method 2 gives $k_{3b}/k_3 \leq 3\%$ for $T_{vib}(OH) = 8400$ K, and $k_{3b}/k_3 \leq 10\%$ for $T_{vib}(OH) = 2000$ K. These temperatures represent reasonable limits given the CO distribution and the exothermicity of the reaction. Considering this uncertainty, the conservative value of $k_{3b}/k_3 \leq 10\%$ is recommended.

A few possible complications in this experiment should be considered. Both CO and CO_2 are products of the reaction CH + O_2, where the CH radicals in this experiment arise from photodissociation of HCCO. Recent measurements of CH + O_2 gives product branching fractions of 30% for CO_2 and 50% for CO.[22] The rate coefficient for this reaction at 300 K is 4.7×10^{-11} cm^3 molecule^{-1} s^{-1},[23] significantly faster than that for the title reaction. Under the range of O_2 concentrations used in this study the time-constants for product formation would range from 2 to 26 μs. There is no evidence for CO or CO_2 production that match this time scale in the present experiments. While the fate of the CH radicals is unknown, the rate coefficient for reaction with ethyl ethynyl ether and with hexane is expected to be approximately an order of magnitude larger than for CH + O_2, and the former reactions are unlikely to produce CO or CO_2. It therefore appears that CH + O_2 has a negligible effect on the experiments presented here. A second possible complication is the effect of vibrational excitation of HCCO on the title reaction. The reaction conditions are chosen so that most of the HCCO radicals are vibrationally thermalized before significant reaction occurs, as evidenced by the loss of emission signal from vibrationally excited HCCO. Because the thermalization rate of HCCO is independent of O_2 concentration, the effect of vibrational excitation on the reaction, if significant, would appear as the O_2 concentration is varied. Under the conditions studied, there is no evidence that the observed reaction product distribution is affected by vibrational excitation of HCCO.

The dominant mechanism proposed in ref 6 for HCCO + O_2 $\rightarrow$ H + CO + CO_2 involves addition of O_2 to the methylidyne carbon, followed by formation of an intermediate with a four-membered COOC ring in which the attacking O_2 bridges the two carbon atoms. Dissociation of this intermediate (without breaking either of the two newly formed bonds) over a small barrier leads to HCO + CO_2, followed by very rapid decomposition of HCO to H + CO. Both the strained four-membered ring and the fact that both newly formed bonds are considerably extended in the intermediate compared to their asymptotic values are consistent with the extremely hot CO and CO_2 internal energy distributions seen in Figure 1b. The noninverted vibrational distribution observed in CO is also consistent with dissociation of an intermediate complex, as opposed to a direct reaction mechanism. To be fair, deposition of large amounts of energy into vibration of the fragments is expected for highly exothermic reactions, such as reaction 3a, and the state distributions may not be a specific indicator of the reaction intermediate. The experimental upper limit on the branching ratio for channel 3b is in agreement with the theoretical results of ref 6.

The authors in refs 9 and 11 tentatively identified reaction 3b producing OH + CO + CO in their experiments. If this were the case, the CO_2 emission observed in the present experiments would have to be rationalized as arising from OH + CO $\rightarrow$ H + CO_2 ($k = 1.25 \times 10^{-13}$ cm^3 molecule^{-1} s^{-1} at 298 K).[24] However, since OH and CO are products of channel 3b, CO_2 production would be a second-order process and could never account for the yield or the rise time of CO_2 observed in the present data.

In summary, the products of the HCCO + O_2 reaction have been observed for the first time and offer a credible explanation for prompt CO_2 observed in acetylene combustion in shock-tube and flame experiments. The results support a recent theoretical paper[6] that proposed a reaction mechanism involving a four-membered ring intermediate that dissociates to yield H + CO + CO_2. No evidence is seen for the product channel OH + CO + CO, but the experiment gives an upper limit for this branching ratio of 10% at 298 K.

Acknowledgment. This research is supported by the Division of Chemical Sciences, Geosciences, and Biosciences, the Office of Basic Energy Sciences of the United States Department of Energy. The author thanks Dr. Stephen Klippenstein and Dr. Jim Miller for helpful discussions, Prof. Richard Bersohn and Prof. Laurie Butler for the suggestion of the HCCO photolytic precursor and sharing of unpublished data, Gary Wilke for technical assistance, and the reviewer for several helpful comments that clarified the discussion, particularly the branching-ratio measurement.

References and Notes

(1) Westbrook, C. K.; Dryer, F. L. *Proc. Combust. Inst.* **1981**, *18*, 749.
(2) Brezinsky, K. *Prog. Energy Combust. Sci.* **1986**, *12*, 1.
(3) Homer, J. B.; Kistiakowsky, G. B. *J. Chem. Phys.* **1967**, *47*, 5290.
(4) Eberius, K. H.; Hoyermann, K.; Wagner, H. Gg. *Proc. Combust. Inst.* **1973**, *14*, 147.
(5) Peeters, J.; Boullart, W.; Langhans, I. *Int. J. Chem. Kinet.* **1994**, *26*, 869. Michael, J. V.; Wagner, A. F. *J. Phys. Chem.* **1990**, *94*, 2453.
(6) Klippenstein, S. J.; Miller, J. A.; Harding, L. B. *Proc. Combust. Inst.*, in press.
(7) Peeters, J.; Schaekers, M.; Vinckier, C. *J. Phys. Chem.* **1986**, *90*, 6552.
(8) Temps, F.; Wagner, H. Gg.; Wolf, M. *Z. Phys. Chem.* **1992**, *176*, 27.
(9) Murray, K. K.; Unfried, K. G.; Glass, G. P.; Curl, R. F. *Chem. Phys. Lett.* **1992**, *192*, 512.
(10) Carl, S. A.; Sun, Q.; Peeters, J. *J. Chem. Phys.* **2001**, *114*, 10332.
(11) Schaekers, M. Ph. D. dissertation, Faculty of Sciences, K. U. Leuven, 1985.
(12) Seakins, P. W. *The Chemical Dynamics and Kinetics of Small Radicals*; Liu, K., Wagner, A., Eds.; World Scientific: Singapore, 1995; pp 250−314.
(13) Krisch, M. J.; Miller, J. L.; Butler, L. J.; Su, H.; Bersohn, R.; Shu, J. *J. Chem. Phys.* **2003**, in press.
(14) Jacox, M. E.; Olson, W. B. *J. Chem. Phys.* **1987**, *86*, 3134.
(15) Unfried, K. G.; Curl, R. F. *J. Mol. Spectrosc.* **1991**, *150*, 86.
(16) Osborn, D. L.; Mordaunt, D. H.; Choi, H.; Bise, R. T.; Neumark, D. M.; Rohlfing, C. M. *J. Chem. Phys.* **1997**, *106*, 10087.
(17) Clifford, E. P.; Farrell, J. T.; DeSain, J. D.; Taatjes, C. A. *J. Phys. Chem. A* **2000**, *104*, 11549.
(18) DeMore, W. B.; Sander, S. P.; Golden, D. M.; Hampson, R. F.; Kurylo, M. J.; Howard, C. J.; Ravishankara, A. R.; Kolb, C. E.; Molina, M. J. *Chemical Kinetics and Photochemical Data for Use in Stratospheric Modeling*; Jet Propulsion Laboratory, Pasadena, CA, 1997.
(19) Park, C. R.; Wiesenfeld, J. R. *J. Chem. Phys.* **1991**, *95*, 8166.
(20) Chackerian, C.; Tipping R. H. *J. Mol. Spectrosc.* **1983**, *99*, 431.
(21) Nelson, D. D.; Schiffman, A.; Nesbitt, D. J. *J. Chem. Phys.* **1989**, *90*, 5455.
(22) Bergeat, A.; Calvo, T.; Caralp, F.; Fillion, J.-H.; Dorthe, G.; Loison J.-C. *Faraday Discuss.* **2001**, *119*, 67.
(23) Taatjes, C. A. *J. Phys. Chem.* **1996**, *100*, 17840.
(24) Baulch, D. L.; Cobos, C. J.; Cox, R. A.; Esser, C.; Frank, P.; Just, Th.; Kerr, J. A.; Pilling, M. J.; Troe, J.; Walker, R. W.; Warnatz, J. *J. Phys. Chem. Ref. Data* **1992**, *21*, 411.